Environ. Sci. Technol. **2003**, *37*, 4894−4900

Effect of Salinity on the Photolysis of Chrysene Adsorbed to a Smectite Clay

LI KONG AND JOHN L. FERRY*

Department of Chemistry and Biochemistry, University of South Carolina, Columbia, South Carolina 29208

The rate of photooxidation (λ, 300−800 nm) of the polycyclic aromatic hydrocarbon chrysene was significantly enhanced in aqueous suspensions of the smectite clay, Laponite RD, relative to its rate of photolysis in aqueous solution. The photodegradation of chrysene is reported at pH 8.30, at several different ionic strengths that correlate to freshwater and saltwater. The kinetics of chrysene loss are first order in chrysene. The photodegradation products 1,4-chrysenediol, 1,4-chrysenequinone, phthalic acid, and 2-formyl benzoic acid have been positively identified and quantified against analytical standards. The mechanism of chrysene degradation was probed by comparing the effects of added methanol, bicarbonate, diazabicyclooctane, chloride, bromide, and iodide on the rate of chrysene photooxidation. Chrysene photooxidation was suppressed by diazabicyclooctane and halide ions but was unaffected by methanol or bicarbonate, implying that $^1O_2$ played a significant role in its removal. The overall rate of chrysene loss was governed by the salinity of the solution and the extent of surface coverage. The steady-state concentration of singlet oxygen was measured and varied positively with chrysene loading but was reduced dramatically at salinities comparable to the marine environment. The relative contributions of Cl^-, Br^-, and I^- to the reduction in $[^1O_2]_{ss}$ are reported, with I^- the most effective $^1O_2$ quencher. The implication of the research is that photoprocessing of particle-bound PAHs may fall off as rapidly as they are transported into marine environments. A predictive kinetic model for the photodegradation of adsorbed chrysene is presented.

Introduction

Polynuclear aromatic hydrocarbons (PAHs) are generated whenever organic materials are heated in low O_2 environments (*1*, *2*). Sources of PAHs in the environment include urban runoff, oil spills, steel and coking operations, and petroleum refining (*3*−*5*). The presence of PAHs is of great concern due to their significant mutagenic and/or carcinogenic activity (*6*, *7*). This toxicity is ascribed not only to the PAHs but also some of their degradation products (*8*−*10*).

The low aqueous solubility of most PAHs drives them to associate with less polar phases such as particulate organic matter, suspended solids, or sediments (*1*, *11*, *12*). Sanger and co-workers studied 28 tidal creeks along the South Carolina coast and found that the concentrations of PAHs were in the following order: creeks with industrial/urban watersheds > suburban watershed > forested watershed (*13*). Elevated concentrations of PAHs have been observed in the surface sediments of the internal-coastal waters with highest concentrations in the intercoastal waterways and estuaries (*14*−*16*). Fine slurries of clays are common in sediments in coastal regions of the southeastern United States, and many organic pollutants are often deposited or adsorbed on their surfaces (*17*, *18*). Although clays rarely display significant intrinsic photocatalytic properties, they do serve as host materials that can promote photochemical reaction of "guests" in a highly confined microenvironment (*19*−*21*). Excellent reviews in this field have been published by Thomas (*22*) and Shichi and Takagi (*23*) in the past decade.

This work is concerned with the manner in which clays affect the photodegradation of adsorbed PAHs, particularly chrysene. It is well-known that the photoexcitation of PAHs can result in the formation of triplet states (^{3}PAH) that can engage in electron or energy transfer reactions (*24*−*26*). In aqueous solution, there is strong evidence that the photooxidation of PAHs is a result of electron transfer between the ^{3}PAH and dissolved oxygen or water (*25*, *27*). However, in organic solvents or on surfaces, it is common for ^{3}PAH to engage in energy transfer with triplet oxygen to generate singlet oxygen, a moderate oxidant (*28*−*30*). In fact, energy transfer between ^{3}PAH and dissolved oxygen under those conditions is essentially a diffusion-controlled process (*24*, *26*, *28*).

PAHs are known to be associated with particulate matter in the water column, a significant portion of which is often suspended clay (*18*, *31*, *32*). Recently, several investigators have been looking at the role of clays as platforms for promoting the photodegradation of micropollutants in the environment. Katagi found that indirect photolysis of tolclofos-methyl (*33*), an organophosphorus fungicide, esfenvalerate (a pyrethroid insecticide) (*34*, *35*), and 3-phenoxybenzoic acid (*36*) occurred in the presence of clay (kaolinite, montmorillonite) suspensions. Mathew et al. found that the rates of photodegradation of metolachlor were faster in the presence of soil minerals (kaolinite, montmorillonite, and goethite) than in water and that the number of photodegradation products formed was higher (*37*). The adsorption of an intrinsically photoactive micropollutant to a surface known to promote photochemical reactions is a compelling phenomena for study. In the southeastern United States, there are several developed estuaries that receive high levels of urban runoff and are also quite turbid, which suggests that surface-promoted photodegradation may be a significant route for PAH oxidation in these environments (*38*−*40*).

Experimental Section

Chemicals. Chrysene (98%), 1,4-chrysenequinone, phthalic acid (99.5%), $NaBH_4$ (98%), 1,4-diazabicyclo[2,2,2]octane (DABCO) (98%), and bis(trimethylsilyl)trifluoroacetamide (BSTFA) (99%) with 1% trimethylchlorosilane (TMCS) were purchased from Aldrich. 2-Formyl benzoic acid (>98%) was purchased from TCI. 2,5-Diphenylfuran was purchased from Alfa Aesar. Laponite RD was donated by Southern Clay Products Inc. (Gonzales, TX). The composition of anhydrous Laponite as supplied by the producer is as follows: SiO_2, 55.6%; MgO, 25.1%; Na_2O, 3.6%; Li_2O, 0.7%; K_2O, 0.2%; TiO_2, 0.15%; Al_2O_3, 0.08%; CaO, 0.06%; Fe2O3, 0.04%. Instant Ocean, NaCl (certified ACS), methanol (GC grade), *n*-pentane (pesticide grade), and acetone (HPLC grade) were supplied by Fisher. Methyl *tert*-butyl ether (MTBE, GC grade) was supplied by Merck KgaA, Germany. NaI (GR) was purchased from EM Science, and KBr (AR) was purchased from

* Corresponding author telephone: (803)777-2646; fax: (803)777-9521; e-mail: ferry@mail.chem.sc.edu.

10.1021/es026124o CCC: $25.00 © 2003 American Chemical Society
Published on Web 09/30/2003

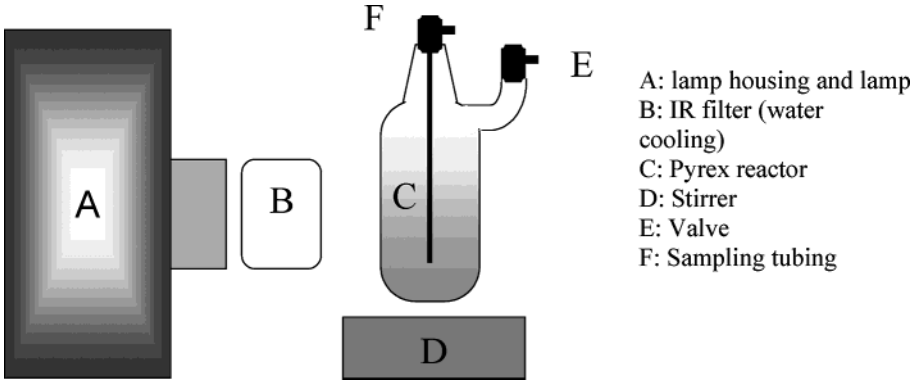

FIGURE 1. Experimental setup for photodegradation of chrysene. Lamp: 1000-W Xe arc lamp, $\lambda_{ex} > 300$ nm, $I_{av} = 2.60 \times 10^{-5}$ einstein/min.

Mallinckrodt Chemicals. The N_2 BET surface area of Laponite RD was 386.6 ± 0.7 m^2/g. Acetone was dried over anhydrous sodium sulfate. All other materials were used as received.

Synthesis of 1,4-Chrysenediol. The synthesis of 1,4-chrysenediol was achieved through the reduction of 1.04×10^{-7} mol of 1,4-chrysenequinone by a 10-fold excess of $NaBH_4$ (*41*) in acetone under N_2. During the reaction, the dark orange color of 1,4-chrysenequinone slowly faded to yield a clear solution. Following reduction, the air-sensitive 1,4-chrysenediol was immediately derivatized with BSTFA (*42*). Acetone was removed by evaporation under nitrogen, and the residue was taken up in MTBE for analysis by GC/MS (EI, CI, MS/MS).

Experimental Setup. The reactor used in all experiments was an ACE glass Pyrex reactor (Figure 1). The light source was a 1000-W Xe arc lamp (Oriel 68820 power supply and Oriel 66021 lamp housing) equipped with a 10 cm long Pyrex water-cooled IR filter. The irradiation wavelength was 300 nm $< \lambda_{ex} <$ 800 nm, and the integrated light intensity over the range of 300−500 nm was 2.6×10^{-5} einstein/min. Lamp output was monitored over time by ferrioxalate actinometry (*43*).

Methods. All handling of chrysene solutions was done under yellow light. Adsorption of chrysene onto Laponite was achieved by adding Laponite to a stock solution of chrysene in *n*-pentane and allowing it to equilibrate with stirring for 15 min. Pentane was then removed by gentle rotary evaporation. This method is consistent with the approach of Reyes and co-workers (*44*). Chrysene loading was determined by extracting chrysene from the Laponite (total chrysene in all experiments exceeded its solubility by a factor of >30) and determined by measuring chrysene by GC/MS techniques (*44*). Chrysene-loaded Laponite was used for all heterogeneous suspension experiments. Co-adsorbed DABCO or 2,5-diphenylfuran was achieved by adding Laponite into a pentane stock solution of both DABCO and chrysene or 2,5-diphenylfuran and chrysene to the desired molar ratio, following similar steps as the chrysene loading on Laponite.

For solution-phase photochemical studies, aqueous methanolic chrysene was prepared by spiking 10.00 mL of chrysene in methanol stock solution into 90.00 mL of buffer or simulated seawater (Instant Ocean) at the desired salinity, making the final irradiated solution 10% MeOH. This approach is consistent with the work of Miller and Olejnik (*45*). The corresponding heterogeneous experiments were prepared by taking up Laponite precoated with chrysene into 100 mL of buffer or simulated seawater with different salinity and mixing vigorously.

All experiments were allowed to equilibrate in the dark with stirring for 50 min before illumination. pH was monitored during equilibration and was adjusted to 8.30 (representative of most marine waters) with 0.1 M HCl or NaOH. After equilibration, the lamp was ignited, and illumination of the reactor commenced when lamp output stabilized (15 min after the light was on). Samples (2 mL) were removed from the top sample port with a 4-mL spring-loaded syringe (Manostat). Samples were immediately placed in EPA vials precharged with 2 mL of MTBE (with triphenylmethane internal standard). Samples were sonicated for 10 min (*44*) and then extracted on a vortex mixer for 1min. The organic layer was removed and stored at 4 °C until analysis by GC/MS.

Instrumental. Fluorescence spectra were recorded by a SLM-Aminco model 8100 spectrofluorometer (Spectronic Instruments, Rochester, NY) equipped with a 450-W ozone-free xenon arc lamp and an R-928 photomultiplier. The slit width for both excitation and emission monochromators was set to give a 2-nm spectral resolution.

All GC analyses were done on a Varian 3800 GC equipped with an 8200 autosampler and a Saturn 2000 IT-MS. The analytical column was J&W DB-5MS (L = 30 m, i.d. = 0.25 mm, df = 0.25μm) column. Carrier gas was He, and the flow rate was 1.3 mL/min. The injector port was set for splitless operation at 250 °C. The autoinjector volume was set at 1 μL. The temperature program was as follows: hold for 2 min at 60 °C, increase at a rate of 10 °C/min to 100 °C, isothermal at 100 °C for 1 min, increase at 15 °C/min to 200 °C, and isothermal for 2 min, increase at 20 °C/min to 280 °C, hold 5min. The transfer line temperature was 270 °C. The full-scan data acquisition was made over the range of 55−500 m/z for EI, CI, and MS/MS. The ion trap conditions for acetonitrile CI mode were as follows: target TIC, 20000 counts; CI maximum ionization time, 2000 ms; CI maximum reaction time, 110 ms; prescan ionization time, 100 μs; CI storage level, 19.0 m/z; and ejection amplitude, 15.0 V. In MS/MS mode conditions were as follows: target TIC, 5000; prescan ionization time, 1500 μs; nonresonant MS/MS ion preparation, single ion isolation with 3.0 m/z isolation window; excitation storage level, 55.0 m/z; and excitation amplitude, 35.00 V.

Product Determination. 1,4-Chrysenequinone was extracted and identified without derivatization. 1,4-Chrysenediol was extracted by MTBE, concentrated by evaporation, redissolved in acetone, and derivatized with BSTFA to yield the derivatized product at room temperature (*42*). 2-Formylbenzoic acid and phthalic acid were extracted at pH 1, and then the organic extract was derivatized with CH_2N_2 to yield the corresponding methyl esters (*41*, *46*). All were positively identified by comparing their retention time and EI, CI, and MS/MS mass spectra against those of standards.

Results and Discussion

Photodegradation of Chrysene in Solution. Chrysene was irradiated in air-saturated solutions (10/90 mL of methanol/0.001 M $NaHCO_3$ buffer) under a Xe arc lamp with an IR

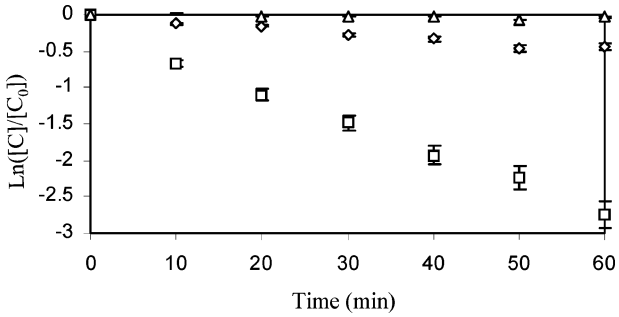

FIGURE 2. Chrysene photolysis is more rapid in the presence of Laponite as compared to the homogeneous solution. Experiments were carried out in 0.001 M $NaHCO_3$ buffer with 10 wt % MeOH: $I_{av} = 2.60 \times 10^{-5}$ einstein/min; pH 8.30. (◇) Photolysis: k_{obs}, (0.63 ± 0.06) × 10^{-2} min^{-1}. (□) Chrysene coated on Laponite: loading, 8.08 μmol/g; Laponite at 1 wt % loading, k_{obs}, (4.35 ± 0.22) × 10^{-2} min^{-1} (no methanol). (△) Photolysis with DABCO, DABCO:chrysene ≈ 10:1.

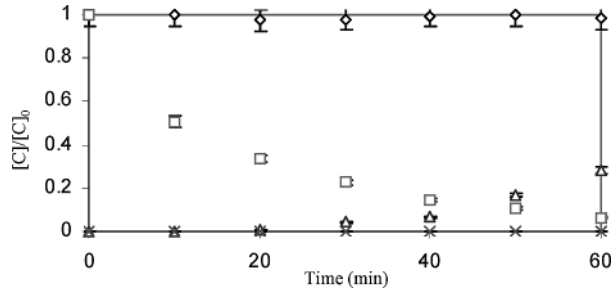

FIGURE 3. Several products were generated during the photodegradation of chrysene on Laponite. Experimental conditions were as follows: 0.001 M $NaHCO_3$ buffer, $I_{av} = 2.60 \times 10^{-5}$ einstein/min; pH 8.30; chrysene loading, 8.08 μmol/g; Laponite 1 wt %. (◇) Chrysene dark control. (□) Chrysene photolysis: k_{obs}, 4.35 × 10^{-2} min^{-1}. (△) Phthalic acid. (×) 1,4-Chrysenequinone.

water filter. This experiment provided the comparative data set against which the effects of the Laponite surface on chrysene could be measured. A small rate of dark loss that is presumed to be sorption of chrysene to the wall of the reactor was observed and subtracted from the total rate under light. Under our experimental conditions, the photodegradation of chrysene was first order in chrysene with a rate constant of (0.63 ± 0.06) × 10^{-2} min^{-1}(Figure 2). Direct photolysis of chrysene in solution only generated trace quantities of products (primarily pthalic acid) detectable by our techniques, with a mass balance of <5% relative to chrysene consumed. Addition of the singlet oxygen scavenger diazabicyclooctane (DABCO) (*47*) at a 10-fold excess (relative to chrysene) halted chrysene photodegradation completely. PAH photodegradation typically can occur through direct photolysis (photoionization or photohydrolysis) (*48*−*50*) or through self-sensitized oxidation by $^1O_2$ (*51*−*53*). It is generally accepted that in solution, at low PAH concentrations (nanomolar), direct photolysis dominates but that at the micromolar concentrations encountered in this study oxidation by singlet oxygen appears to be the more significant pathway. This finding is in agreement with the early models of self-sensitized photooxidation proposed by Lee-Ruff, Eisenberg, and Stevens (*24, 26, 51*−*53*). Under our conditions, using HCO_3^- as the pH adjuster and methanol as the cosolvent, it is unlikely that chrysene degradation could have been the result of some $HO^•$ process (*54, 55*). Many studies have shown that photochemical generation of $^1O_2$ is a widespread phenomenon in the aquatic environment (*56*−*58*). It infers that photodegradation of PAHs in the environment through $^1O_2$ is an important pathway.

Photodegradation of Chrysene on Laponite. Air-saturated aqueous suspensions of Laponite coated with chrysene (submonolayer coverage, 8.08 μmol/g) were buffered at pH 8.30 (0.001 M $NaHCO_3$) and irradiated in an identical manner to the solutions described previously. Chrysene loss was still first order, but it was more rapid than chrysene photolysis in solution (Figure 2) with a first-order rate constant of (4.35 ± 0.22) × 10^{-2} min^{-1}. Heterogeneous photolysis on Laponite resulted in the production of phthalic acid (28.41%), 1,4-chrysenequinone (4.28%), and traces of 1,4-chrysenediol and 2-formylbenzoic acid (Figure 3, yield given in terms of chrysene consumed). There were also several tentatively identified products detected by GC/MS (EI, CI, MS/MS) but not quantified (Figure 4). The role of $^1O_2$ was probed by measuring the rate of chrysene decomposition in the presence of co-adsorbed DABCO (~10:1 DABCO:chrysene). The presence of DABCO reduced the photooxidation rate to (0.10 ± 0.01) × 10^{-2} min^{-1}. This is notable because a comparable amount of DABCO halted the solution-phase photooxidation completely. Presumably, this is because the "concentration" of chrysene adsorbed to the Laponite surface is high relative to that in solution; Stevens and colleagues noted that, at high sensitizer concentrations, it does not appear possible to halt singlet oxygen driven photoperoxidation with scavengers (*24, 26*). When the equivalent amount of DABCO was added to the solution phase of slurries of Laponite coated with chrysene, the same photooxidation was obtained as when they were introduced co-adsorbed. It is probable that the water-soluble DABCO partitioned into the aqueous phase rapidly during the equilibration phase of this experiment. Despite the implication that it is not possible to know (quantitatively) the surface loading of DABCO post-equilibration, both experiments suggest that singlet oxygen retains a significant role in the photodegradation of adsorbed chrysene.

The observation that adsorption onto a surface enhances the rate of PAH photodegradation is well-supported; Sigman and co-workers have reported that the addition of SiO_2 particles to cyclohexane solutions of anthracene increased the rate of anthracene photolysis by a factor of 6.5 under argon and a factor of 56 under oxygen (*59*). Larson and Hunt have also reported dramatic rates enhancements for PAH photodegradation in thin films (*29*). Over the last 10 years, many researchers have reported surface-mediated enhancement of photochemical processes caused by co-adsorption of reactants (*19, 60, 61*).

The rate of chrysene photooxidation varied positively with the extent of chrysene loading, consistent with a self-sensitized process. Chrysene was varied over the range of 1.08−14.00 μmol/g on Laponite. A plot of the inverse of the initial rate versus the inverse of initial concentration from these experiments was linear, with an r^2 of 0.97 and k of 0.38 μmol g^{-1} min^{-1} (Figure 5). The emission spectrum (see Supporting Information Figure 1) of the suspension was taken and found to be essentially the same as that of chrysene in solution. The typical excimer emission band of PAHs (470−600 nm) (*62, 63*) was not observed, which was interpreted as an indication that chrysene was not close-packed or stacked on the surface.

Effect of Common Anions on Chrysene Degradation. Heterogeneous suspensions of chrysene coated on Laponite (5.25 μmol/g) were also irradiated in simulated seawater at different salinities and also in solutions of individual anions at concentrations representative of their concentration in seawater (Table 1). It was observed that all anions depressed the rate of chrysene photooxidation. The falloff in k_{obs} as a function of salinity is quite rapid; it decreases by a factor of 10 over the salinity range of 0−10‰ (Figure 6). Speculatively, this is due to quenching of $^1O_2$, quenching of chrysene* (both singlet and triplet chrysene) (*64*), or some combination thereof. The relative role of $^1O_2$ quenching versus chrysene* quenching is discussed below.

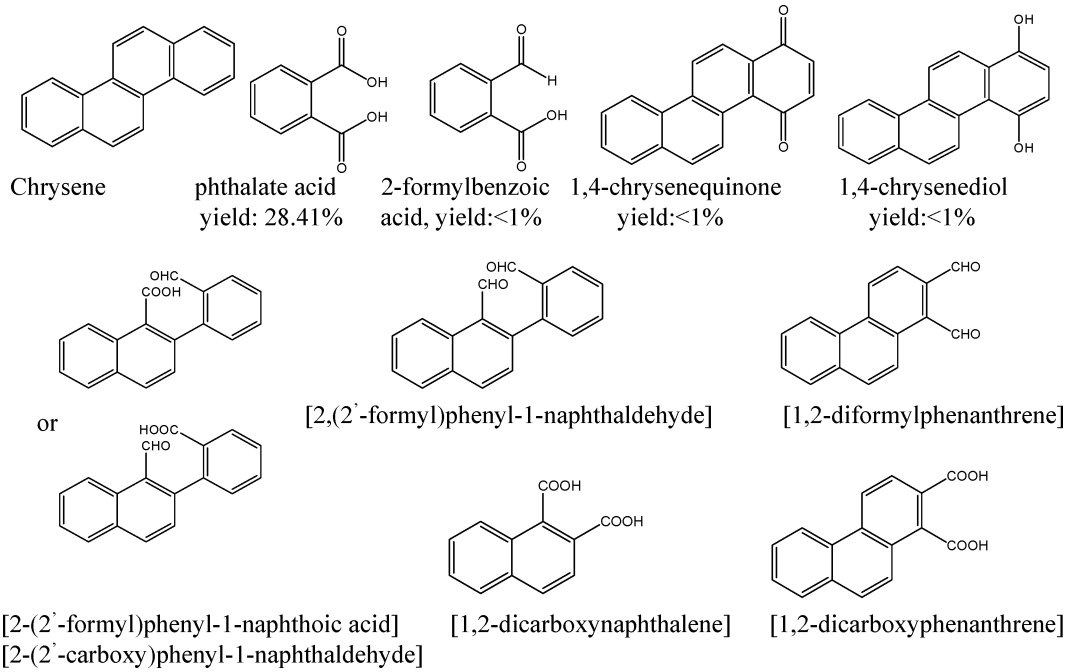

FIGURE 4. Positively and [tentatively] identified products.

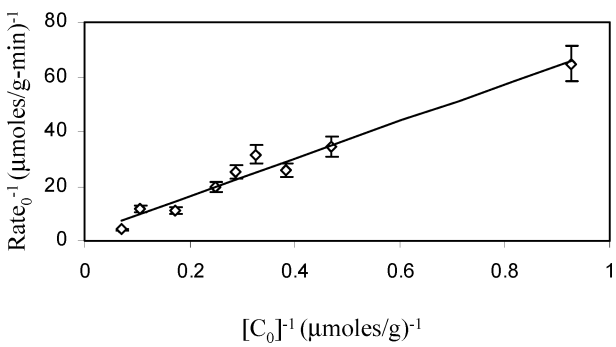

FIGURE 5. Reciprocal initial rate (R_0^{-1}) vs reciprocal initial chrysene concentration ($[C_0]^{-1}$) 0.001 M $NaHCO_3$ buffer: $I_{av} = 2.60 \times 10^{-5}$ einstein/min; pH 8.30; Laponite 1 wt %.

Kinetic Model. Results of the DABCO experiments suggested that $^1O_2$ was the most probable oxidant in this system. Accordingly, a $^1O_2$-based model was developed as a tool for predicting the photolysis rate of particle-bound chrysene in the presence of common anions. Assuming that chrysene (singlet and triplet) catalyzes its own oxidation by the production of $^1O_2$, a simplified reaction scheme can be used to describe the system (*28*−*30*):

$$\text{Chry} \xrightarrow{h\nu, I_a} \text{Chry*} \tag{1}$$

$$\text{Chry*} + {}^3O_2 \xrightarrow{\Phi} \text{Chry} + {}^1O_2 \tag{2}$$

$${}^1O_2 \xrightarrow{k_d} {}^3O_2 \qquad k_d = (2.5 \times 10^5\ s^{-1})\ (65) \tag{3}$$

$${}^1O_2 + S \xrightarrow{k_q} {}^3O_2 + S \tag{4}$$

$${}^1O_2 + \text{Chry} \xrightarrow{k_r} \text{products} \tag{5}$$

where I_a is the rate of light absorption by chrysene, Φ is the quantum efficiency for sensitized $^1O_2$ production (assuming an air-saturated solution), k_d is the first-order rate constant for physical quenching of $^1O_2$ by water, k_q is the second-order rate constant for physical quenching of $^1O_2$ by the generic $^1O_2$ scavengers S (a term that includes chrysene), and k_r is the second-order rate constant for the chemical reaction between $^1O_2$ and chrysene. Under continuous irradiation, and assuming the loss of chrysene was dependent on singlet oxygen, the following rate law can be derived for a well-mixed system:

$$-\frac{d[\text{Chry}]}{dt} = k_r[{}^1O_2][\text{Chry}] \tag{6}$$

The steady-state approximation for $[^1O_2]$ is

$$-\frac{d[{}^1O_2]_{ss}}{dt} = I_a\Phi - k_d[{}^1O_2]_{ss} - (k_r + k_q)[{}^1O_2]_{ss}[\text{Chry}] = 0 \tag{7}$$

Rearranging eq 7 yields

$$[{}^1O_2]_{ss} = \frac{I_a\Phi}{k_d + (k_r + k_q)[\text{Chry}]} \tag{8}$$

according to the Beer−Lambert law:

$$c = [\text{Chry}]_0:\ I_a = I_0(1 - e^{-\epsilon bc}) \tag{9}$$

so, if $\epsilon bc \ll 1$, eq 9 can be simplified to

$$I_a = I_0\epsilon b[\text{Chry}]_0 \tag{10}$$

Substituting eq 10 into eq 8 yields

$$[{}^1O_2]_{ss} = \frac{(I_0\epsilon b)\Phi[\text{Chry}]_0}{k_d + (k_r + k_q)[\text{Chry}]} \tag{11}$$

Since the value of k_d for $^1O_2$ is $2.5 \times 10^5\ s^{-1}$ (*65*) and the maximum initial concentration of chrysene in this work was 1.33×10^{-4} M, k_d will be much greater than the term (k_r +

TABLE 1. Effect of Common Anions on Chrysene Degradation

systems[a]	$k_{obs} \times 10^{-2}$ (min^{-1})	$k_{obs}/k_{obs(index)}$	$t_{1/2}$ (h)[b]	est of environ half-life (h)[c]	k_{Chry^*,X^-} ($M^{-1}\ s^{-1}$)[d]
0.001 M $NaHCO_3$	1.90 ± 0.10	1	0.61	4.45	
0.001 M $NaHCO_3$ + 28.78 μM KBr[e]	1.45 ± 0.07	0.76	0.80	5.83	8.34×10^3
0.001 M $NaHCO_3$ + 1.73 μM NaI[e]	1.42 ± 0.07	0.75	0.81	5.96	1.44×10^5
0.001 M $NaHCO_3$ + 0.543 M NaCl[e]	0.57 ± 0.03	0.30	2.03	14.8	1.29
instant seawater (salinity of 34‰)	0.07 ± 0.01	0.04	16.50	120	

[a] Chrysene loading: 5.25 μmol/g with different salinity, $I_{av} = 2.60 \times 10^{-5}$ einstein/min; pH 8.30. [b] $t_{1/2} = \ln 2/k_{obs}$. [c] Normalization of our light intensity to average intensity of sunlight for a clear summer day is based on the Yager and Yue (*75*) measurement. [d] Estimated k_{Chry^*,X^-} from eq 22. X^-: common anions in seawater, Cl^-, Br^-, I^-. [e] Concentrations of each ion are representative of their molarities in 34‰ seawater.

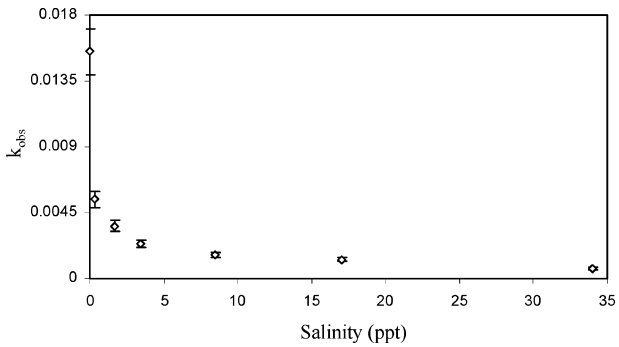

FIGURE 6. Increasing salinity results in the suppression of chrysene photodegradation on Laponite suspensions. All experiments were carried out in 0.001 M $NaHCO_3$ buffer (0 salinity) and simulated seawater with different salinity, $I_{av} = 2.60 \times 10^{-5}$ einstein/min; pH 8.30; chrysene loading, 3.96 μmol/g; Laponite 1 wt %.

k_q)[Chry]. Assuming this to be the case, the steady-state concentration of $^1O_2$ can be expressed as

$$[^1O_2]_{ss} = \frac{I_0 \epsilon b \Phi}{k_d}[\mathrm{Chry}]_0 \quad (12)$$

The substitution of eq 12 into eq 6 yields

$$-\frac{d[\mathrm{Chry}]}{dt} = k_r \frac{I_0 \epsilon b \Phi [\mathrm{Chry}]_0}{k_d}[\mathrm{Chry}] \quad (13)$$

Since the reaction is first order in chrysene, it is simplified to

$$-\frac{d[\mathrm{Chry}]}{dt} = k_r[^1O_2]_{ss}[\mathrm{Chry}] = k_{obs}[\mathrm{Chry}] \quad (14)$$

where k_{obs} is the pseudo-first-order rate constant defined by

$$k_{obs} = k_r[^1O_2]_{ss} \quad (15)$$

However, this model was incapable of fully predicting the effect of $^1O_2$ scavengers on k_{obs}. The addition of halides can depress the rate of chrysene degradation by quenching $^1O_2$ or chrysene* directly. There is a great deal of literature precedent for quenching of excited states by halide ions, through collisional and electron-transfer processes (*64*, *66*, *67*). Accordingly, the model was modified to take into account direct quenching of chrysene* as well as $^1O_2$ by halide ions. The refined model incorporated the following reactions:

$$^1O_2 + X^- \xrightarrow{k_{r,X^-}} \text{products} \quad (16)$$

$$\mathrm{Chry}^* + X^- \xrightarrow{k_{Chry^*,X^-}} \mathrm{Chry} + \text{products} \quad (17)$$

yielding a more refined expression for $[^1O_2]_{ss}$:

$$[^1O_2]_{ss} = \frac{I_0(1 - \sum(k_{Chry^*,X^-}[X^-]))\epsilon b \Phi [\mathrm{Chry}]_0}{k_d + \sum(k_{r,X^-}[X^-]) + (k_r + k_q)[\mathrm{Chry}]} \quad (18)$$

Equation 18 was simplified to

$$[^1O_2]_{ss} = \frac{I_0(1 - \sum(k_{Chry^*,X^-}[X^-]))\epsilon b \Phi [\mathrm{Chry}]_0}{k_d + \sum(k_{r,X^-}[X^-])} \quad (19)$$

where k_{r,Br^-}: $< = 10^6$ (L $mol^{-1}\ s^{-1}$) (*68*), k_{r,I^-}: 7.2×10^6 (L $mol^{-1}\ s^{-1}$) (*69*), and k_{r,Cl^-}: 10^3(L $mol^{-1}\ s^{-1}$) (*70*).

2,5-Diphenylfuran (a singlet oxygen trapping agent, $k_r = 4.6 \times 10^7\ M^{-1}\ s^{-1}$ (*71*)) was co-adsorbed on Laponite with chrysene, and this probe was used to measure $[^1O_2]_{ss}$ as a function of chrysene loading. $[^1O_2]_{ss}$ varied positively with chrysene loading in buffer and seawater, although the slope is not as pronounced in seawater ($[^1O_2]_{ss} = 2.30[\mathrm{Chry}]_0 \times 10^{-12}$ M in 0.001 M $NaHCO_3$ buffer and $[^1O_2]_{ss} = 0.90[\mathrm{Chry}]_0 \times 10^{-12}$ M in simulated seawater, Figure 7). Since 2,5-diphenylfuran underwent some direct photolysis, the k_{obs} used for $[^1O_2]_{ss}$ is adjusted by $k_{obs} = k_{obs(\mathrm{chrysene + 2,5-diphenylfuran})} - k_{obs(\mathrm{2,5-diphenylfuran})}$. These trends are consistent with the assumption of eqs 11 and 18 that $[^1O_2]_{ss}$ is proportional to the initial concentration of chrysene. The experiments show that the $[^1O_2]_{ss}$ in $NaHCO_3$ buffer is 2.54 times that in simulated seawater on Laponite. This value is qualitatively consistent with eq 19 and consistent with the ratio of experimental rate constants (Table 1) since the different anions act as scavengers in the system. Since singlet oxygen has relatively poor vibrational overlap with D_2O relative to H_2O, its lifetime in pure D_2O is much longer than in H_2O (20 μs vs 2 μs (*72*)). To verify the role of $^1O_2$ in 2,5-diphenylfuran photooxidation, D_2O was added and $[^1O_2]_{ss}$ was quantified over a range of D_2O concentrations (0−60%) (Figure 8). These experiments showed that chrysene catalyzed the photooxidation of 2,5-diphenylfuran with much higher efficiencies (a factor of ∼55) at high D_2O loadings, implying that singlet oxygen was produced by adsorbed chrysene.

With verification of the role of $^1O_2$, it becomes possible to substitute eq 19 into eq 6 to yield

$$-\frac{d[\mathrm{Chry}]}{dt} = k_r \frac{I_0(1 - \sum(k_{Chry^*,X^-}[X^-]))\epsilon b \Phi [\mathrm{Chry}]_0}{k_d + \sum(k_{r,X^-}[X^-])}[\mathrm{Chry}] \quad (20)$$

Integrating eq 20 yields

$$\ln[\mathrm{Chry}] = k_r \frac{I_0(1 - \sum(k_{Chry^*,X^-}[X^-]))\epsilon b \Phi [\mathrm{Chry}]_0}{k_d + \sum(k_{r,X^-}[X^-])} t + \ln [\mathrm{Chry}]_0 \quad (21)$$

It is apparent that the decrease in $[^1O_2]_{ss}$ with increasing salinity is nonlinear, which is consistent with the hypothesis that halides quench the oxidation of chrysene by scavenging

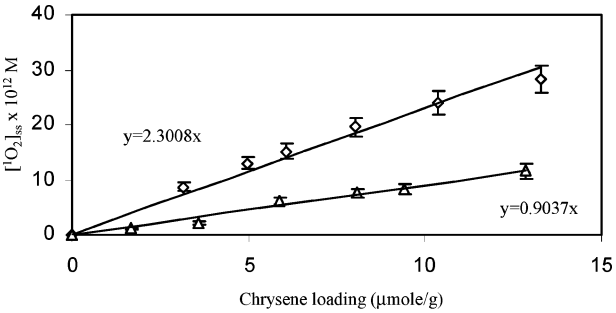

FIGURE 7. $[^1O_2]_{ss}$ (M) varies with chrysene loading on Laponite: (◇) 0.001 M $NaHCO_3$ buffer; (△) Instant Ocean; $I_{av} = 2.60 \times 10^{-5}$ einstein/min; pH 8.30; 2,5-diphenylfuran loading: 49.32 μmol/g; Laponite 1 wt %.

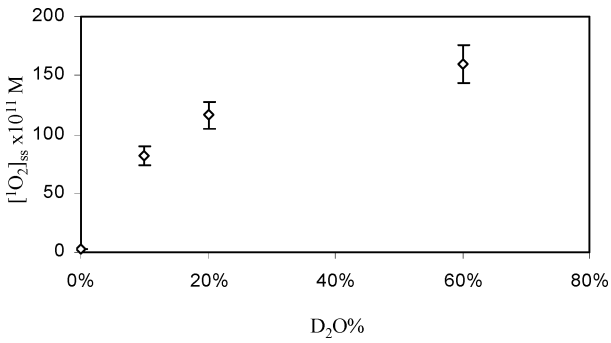

FIGURE 8. Effect of D_2O% on $[^1O_2]_{ss}$ (M), $I_{av} = 2.60 \times 10^{-5}$ einstein/min; pH 8.30; chrysene loading, 5.56 μmol/g; Laponite 1 wt %.

a transient species such as singlet oxygen. When seawater is "deconstructed" into solutions of NaI, NaBr, and NaCl, it is apparent that additively these three species can account for essentially all the quenching effect observed in seawater (Table 1).

Halides are known to adsorb only poorly to some clays (*73*, *74*). If it is assumed that all quenching is the result of reaction between $^1O_2$ and solution-phase halide, it is possible to estimate the bimolecular rate constant for the reaction between these species.

Taking the ratio of k_{obs} from various halide solutions to k_{obs} for 0.001 M $NaHCO_3$ buffer yields

$$\frac{k_{obs}(\text{halides})}{k_{obs}(\text{buffer})} = \frac{k_d(1 - \sum(k_{Chry^*,X^-}[X^-]))}{k_d + \sum(k_{r,X^-}[X^-])} \qquad (22)$$

Applying eq 22 to the experimental data set for the individual anion allows the estimation of k_{Chry^*,X^-} (Table 1).

The integrated rate law (eq 21) allows estimation of the effects of light intensity, initial surface loading, and salinity on the photooxidation of chrysene. The predictions of the proposed kinetic model showed good general agreement with experimental data. Combination of $[^1O_2]_{ss}$ and the chrysene degradation rate constant in different systems allowed a qualitative evaluation of the photochemical fate of particle-bound chrysene at the freshwater–saltwater interface. This will be helpful in predicting PAH photodegradation in dynamic coastal environments.

Acknowledgments

This research was sponsored by U.S. EPA Grant R827397. The authors express gratitude to Prof. Catherine J. Murphy and Prof. Michael Angel for the use of spectroscopic equipment and thank Richard G. Zepp and Richard A. Larson for helpful discussions of portions of this paper.

Supporting Information Available

One table and six figures. This material is available free of charge via the Internet at http://pubs.acs.org.

Literature Cited

(1) Neff, J. M. *Polycyclic Aromatic Hydrocarbons in the Aquatic Environment: Sources, Fates and Biological Effects*; Applied Science: London, 1979.
(2) Zepp, R. G.; Macko, S. A. Series I: Global Environmental Change. *NATO ASI Ser.* **1997**, *No. 51*, 145–166.
(3) Bowling, J. W.; Leversee, G. J.; Landrum, P. F.; et al. *Aquat. Toxicol.* **1983**, *3*, 79–90.
(4) Landrum, P. F.; Scavia, D. *Can. J. Fish. Aquat. Sci.* **1983**, *40*, 298–305.
(5) Newsted, J. L.; Giesy, J. P. *Environ. Toxicol. Chem.* **1987**, *6*, 445–461.
(6) Becedas, L.; Romert, L.; Toft, E.; Jenssen, D. *Reprod. Toxicol.* **1993**, *7*, 219–224.
(7) Warshawsky, D. B.; Barkley, W.; Bingham, E. *Fundam. Appl. Toxicol.* **1993**, *20*, 376–382.
(8) Vo-Dinh, T. *Chemical Analysis of Polycyclic Aromatic Compounds*; Wiley: New York, 1989; Vol. 101.
(9) Clemons, J. H.; Allan, L. M.; Marvin, C. H.; Wu, Z.; Mccarry, B. E.; Bryant, D. W.; Zacharewski, T. R. *Environ. Sci. Technol.* **1998**, *32*, 1853–1860.
(10) U.S. Environmental Protection Agency. EPA-440/4-79-029; U.S. EPA: Washington, DC, 1979.
(11) Andelman, J. B.; Snodgrass, J. E. *Crit. Rev. Environ. Control* **1974**, *4*, 69–83.
(12) Harrison, R. M.; Perry, R.; Wellings, R. A. *Water Res.* **1975**, *9*, 331–346.
(13) Sanger, D. M.; Holland, A. F.; Scott, G. I. *Arch. Environ. Contam. Toxicol.* **1999**, *37*, 458–471.
(14) Witt, G.; Trost, E. *Acta Hydrochim. Hydrobiol.* **1999**, *27*, 308–315.
(15) Khim, J. S.; Lee, K. T.; Kannan, K.; Villeneuve, D. L.; Giesy, J. P.; Koh, C. H. *Arch. Environ. Contam. Toxicol.* **2001**, *40*, 141–150.
(16) Zheng, G.; Man, B. W.; Lam, J. C. W.; Lam, M. H. W.; Lam, P. K. S. *Water Res.* **2001**, *36*, 1457–1468.
(17) Schulthess, C. P.; Huang, C. P. *Soil Sci. Soc. Am. J.* **1991**, *55*, 34–42.
(18) Rebhun, M.; Kalabo, R.; Grossman, L.; et al. *Water Res.* **1992**, *26*, 79–84.
(19) Thomas, J. K. *J. Phys. Chem.* **1987**, *91*, 267–276.
(20) Gafney, H. D. *Coord. Chem. Rev.* **1990**, *104*, 113–141.
(21) Shield, S. R.; Harris, J. M. *J. Phys. Chem. B* **2000**, *104*, 8527–8535.
(22) Thomas, J. K. *Chem. Rev.* **1993**, *93*, 301–320.
(23) Shichi, T.; Takagi, K. *J. Photochem. Photobiol. C: Photochem. Rev.* **2000**, *1*, 113–130.
(24) Stevens, B.; Perez, S. R.; Ors, J. A. *J. Am. Chem. Soc.* **1974**, *96*, 6846–6850.
(25) Fasnacht, M. P.; Blough, N. V. *Environ. Sci. Technol.* **2002**, *36*, 4364–4369.
(26) Stevens, B.; Ors, J. A.; Pinsky, M. L. *Chem. Phys. Lett.* **1974**, *27*, 157–160.
(27) Zepp, R. G., Schlotzhauer, P. F., Jones, P. W., Leber, P., Eds. *Polynuclear Aromatic Hydrocarbons: Third International Symposium on Chemistry and Biology—Carcinogenesis and Mutagenesis*; Ann Arbor Science Publishers: Ann Arbor, MI, 1979; pp 141–158.
(28) Foote, C. S. *Acc. Chem. Res.* **1968**, *1*, 104–110.
(29) Larson, R. A.; Hunt, L. L. *Photochem. Photobiol.* **1978**, *28*, 553–555.
(30) Eisenberg, W. C.; Taylor, K.; Murray, A. W. *Carcinogenesis* **1984**, *5*, 1095–1096.
(31) Herut, B.; Gavrieli, I.; Halicz, L. *Appl. Geochem.* **1997**, *12*, 497–505.
(32) Chester, R. *Bull. Inst. Geol. Bassin Aquitaine* **1982**, *31–32*, 325–335.
(33) Katagi, T. *J. Agric. Food Chem.* **1990**, *38*, 1595–1600.
(34) Katagi, T. *J. Agric. Food Chem.* **1993**, *41*, 2178–2183.
(35) Katagi, T. *J. Agric. Food Chem.* **1991**, *39*, 1351–1356.
(36) Katagi, T. *J. Agric. Food Chem.* **1992**, *40*, 1269–1274.
(37) Mathew, R.; Khan, S. U. *J. Agric. Food Chem.* **1996**, *44*, 3996–4000.
(38) Miller, G. C.; Zepp, R. G. *Environ. Sci. Technol.* **1979**, *13*, 860–863.
(39) Miller, G. C.; Zepp, R. G. *Water Res.* **1979**, *13*, 453–459.
(40) Zepp, R. G.; Schlotzhauer, P. F. *Environ. Sci. Technol.* **1983**, *17*, 462–468.

(41) Vollhardt, K. P. C. *Organic Chemistry*; W. H. Freeman & Company: New York, 1987.
(42) Li, D.; Park, J.; Oh, J. R. *Anal. Chem.* **2001**, *73*, 3089−3095.
(43) Fitzgerald, J. M., Ed. *Analytical Photochemistry and Photochemical Analysis*; Marcel Dekker: New York, 1971.
(44) Reyes, C. A.; Medina, M.; Crespo-Hernandez, C.; et al. *Environ. Sci. Technol.* **2000**, *34*, 415−421.
(45) Miller, J. S.; Olejnik, D. *Water Res.* **2001**, *35*, 233−243.
(46) Ngan, F.; Ikesaki, T. *J. Chromatogr.* **1991**, *537*, 385−395.
(47) Lion, Y.; Gandin, E.; Van de Vorst, A. *Photochem. Photobiol.* **1980**, *31*, 305−309.
(48) Larson, R. A.; Hunt, L. L.; Blankenship, D. W. *Environ. Sci. Technol.* **1977**, *11*, 492−496.
(49) Larson, R. A.; Bott, T. L.; Hunt, L. L.; Rogenmuser, K. *Environ. Sci. Technol.* **1979**, *13*, 965−969.
(50) Wang, C. X.; Yediler, A.; Peng, A.; Kettrup, A. *Chemosphere* **1995**, *30*, 501−510.
(51) Lee-Ruff, E.; Kazarians-Moghaddam, H.; Katz, M. *Can. J. Chem.* **1986**, *64*, 1297−1303.
(52) Eisenberg, W. C.; Desilva, M. *Tetrahedron Lett.* **1990**, *31*, 5857−5860.
(53) Eisenberg, W. C.; Anand, J.; Wang, S. K.; et al. *Photochem. Photobiol.* **1992**, *56*, 441−445.
(54) Buxton, G. V.; Wood, N. D.; Dyster, S. *J. Chem. Soc., Faraday Trans. 1* **1988**, *84*, 1113−1121.
(55) Buxton, G. V.; Greenstock, C. L.; Helman, W. P.; Ross, A. B. *J. Phys. Chem. Ref. Data* **1988**, *17*, 513−886.
(56) Zepp, R. G.; Wolfe, N. L.; Baughman, G. L.; Hollis, R. C. *Nature* **1977**, *267*, 421−423.
(57) Haag, W. R.; Hoigne, J.; Gassman, E.; Braun, A. M. *Chemosphere* **1984**, *13*, 641−650.
(58) Haag, W. R.; Hoigne, J. *Environ. Sci. Technol.* **1986**, *20*, 341−348.
(59) Sigman, M. E.; Zingg, S. P. In *Aquatic and Surface Photochemistry*; Helz, G. R., Zepp, R. G., Crosby, D. G., Eds.; Lewis Publishers: Boca Raton, FL, 1994; pp 197−206.
(60) Anpo, M. *Res. Chem. Intermed.* **1989**, *11*, 67−106.
(61) Anpo, M.; Nishiguchi, H.; Fujii, T. *Res. Chem. Intermed.* **1990**, *13*, 73−102.
(62) Ishida, H.; Takahashi, H.; Sato, H.; Tsubomura, H. *J. Am. Chem. Soc.* **1970**, *92*, 275−280.
(63) Ingle, J. D. J.; Crouch, S. R. *Spectrochemical Analysis*; Prentice-Hall: Upper Saddle River, NJ, 1988.
(64) Knor, G. *Chem. Phys. Lett.* **2000**, *330*, 383−388.
(65) Rodgers, M. A. J.; Snowden, P. T. *J. Am. Chem. Soc.* **1982**, *104*, 5541−5543.
(66) Fenical, W.; Kearns, D. R.; Radlick, P. *J. Am. Chem. Soc.* **1969**, *91*, 7771.
(67) Aloisi, G. G.; Favaro, G. *J. Chem. Soc., Perkin Trans. 2* **1976**, *4*, 456−460.
(68) Rosenthal, I.; Frimer, A. *Photochem. Photobiol.* **1976**, *23*, 209−211.
(69) Rohatgi-Mukherjee, K. K.; Gupta, A. K. *Chem. Phys. Lett.* **1977**, *46*, 368−371.
(70) Egorov, S. Y.; Krasnovsky, A. A. *Sov. Plant Physiol.* **1986**, *33*, 5−8.
(71) Young, R. H.; Brewer, D.; Keller, R. A. *J. Am. Chem. Soc.* **1973**, *95*, 375−379.
(72) Turro, N. J. *Modern Molecular Photochemistry*; Addison-Wesley: Reading, MA, 1978; Chapter 14.
(73) Bolt, G. H., Ed. *Soil Chemistry B: Physico-chemical Models*; Elsevier Scientific: New York, 1979.
(74) Kaplan, D. I.; Serne, J. R.; Parker, K. E.; Kutnyakov, I. V. *Environ. Sci. Technol.* **2000**, *34*, 399−405.
(75) Yager, J. E.; Yue, C. D. *Environ. Toxicol. Chem.* **1988**, *7*, 1003−1011.

Received for review September 5, 2002. Revised manuscript received August 9, 2003. Accepted August 15, 2003.

ES026124O